Modelling of Forward Fall on Outstretched Hands as a System with Ground Contact

Paweł Biesiacki, Jerzy Mrozowski, Dariusz Grzelczyk and Jan Awrejcewicz

Abstract Forward falls on outstretched hands are caused by unexpected lost of stability and they are always related with different kinds of injuries. This paper takes attempt to explain and figure out the multifaceted problems of forward fall. In order to estimate the critical value of the force acting on the hands at the moment of impact on the ground, the relative simple mechanical model is proposed. Mathematical model is described by the second order differential equations obtained by the Newton–Euler method, and its parameters are identified and validated using experimental data from one of the recent paper. Some interesting results are obtained, presented and discussed. The presented numerical simulations show that the proposed model demonstrate good accordance with real tested objects presented in the literature. The model predicts the highest impact force and finally allows to simulate various scenarios of human falls.

1 Introduction

Slips, Trips and Falls (STF) are the highest single cause of upper limb injuries. Falls occur in all age groups and the falls on the outstretched hand are a significant cause of upper limb injury including 90 % of fracture at the distal radius region [1]. A forward fall is the most common type of fall and more than half of the falls among

P. Biesiacki (✉) · J. Mrozowski · D. Grzelczyk · J. Awrejcewicz
Department of Automation, Biomechanics and Mechatronics,
Lodz University of Technology, 1/15 Stefanowski Street,
90-924 Lodz, Poland
e-mail: 800045@p.lodz.pl

J. Mrozowski
e-mail: jerzy.mrozowski@p.lodz.pl

D. Grzelczyk
e-mail: dariusz.grzelczyk@p.lodz.pl

J. Awrejcewicz
e-mail: jan.awrejcewicz@p.lodz.pl

J. Awrejcewicz (ed.), *Dynamical Systems: Modelling*, Springer Proceedings in Mathematics & Statistics 181, DOI 10.1007/978-3-319-42402-6_6

the elderly occur in the forward direction. An attempt to determine the biomechanical factors which have the greatest influence on the risk of injury has been made in [2]. On the basis of impact forces measured during low-height forwards falls onto the outstretched hand, a two degrees of freedom, lumped-parameter mathematical model reflecting the real impact forces has been created. Computer simulations in ADAMS (multibody dynamics simulation software created originally by Mechanical Dynamics Incorporated and then developed by MSC Software Corporation) was used to predict the extent to which age-related muscle atrophy may adversely affect the safe arrest of a forward fall onto the arms. The biomechanical factors affecting the separate risks for wrist fracture or head impact is examined using a two-dimensional, 5-link, forward dynamic model [3]. In reference [4] other two degree of freedom discrete impact model is constructed through system identification and validated using experimental data, in order to understand the dynamic interactions of various biomechanical parameters in bimanual forward fall arrests. To evaluate a worst case scenario well-known falling situations of snowboarders are modelled in paper [5] in different falling scenarios of snowboarders and simulated in order to calculate the resulting loads in the upper extremity. In the mentioned paper numerical simulations are carried out using the multi body dynamics software package SIMPACK 9.0 (SIMPACK AG, Wessling, Germany). The backward fall on outstretched joints of the upper extremity is evaluated as worst case scenario. In reference [6] numerical model of upper limb constructed from computed tomography (CT) data under load of real contact force using Finite Element Method (FEM) is calculated in order to obtain stress distribution and evaluate the most risk areas of fracture bones. In turn, a three degree of freedom mathematical model of human body during forward fall on outstretched hands is presented in [7], where dynamical forces acting on the human parts are obtained by solving the appropriate second order differential equations of motion. Also many other papers have shown utilizing spring-damper to contact modelling of human parts with the ground in various types of motion (for instance, see references [8–11]). Motivated by the references mentioned in this paper, we present a dynamic model with "soft" spring-damper contact which allows to predict ground reaction force in different scenario of human fall.

2 Model of the Biomechanical System

The human forward fall on outstretched hands is schematically presented in Fig. 1. The main assumption for working out the appropriate mathematical model is to take into account flat two degrees of freedom mechanical model.

In Fig. 1, the angle $\varphi_1(t)$ denotes the angle between horizontal x axis and the longitudinal axis of the body 1. The angle $\varphi_2(t)$ is the angle measured from the axis of the body 1 to the axis of the body 2 (its value is defined in the range from 0 to 90 degrees and increases during falling). Parameters a_1 and a_2 denote distances between the centres of mass and rotation axes for bodies 1 and 2, respectively, l_1 is a distance form support point to shoulder joint and l_2 is whole length of the upper

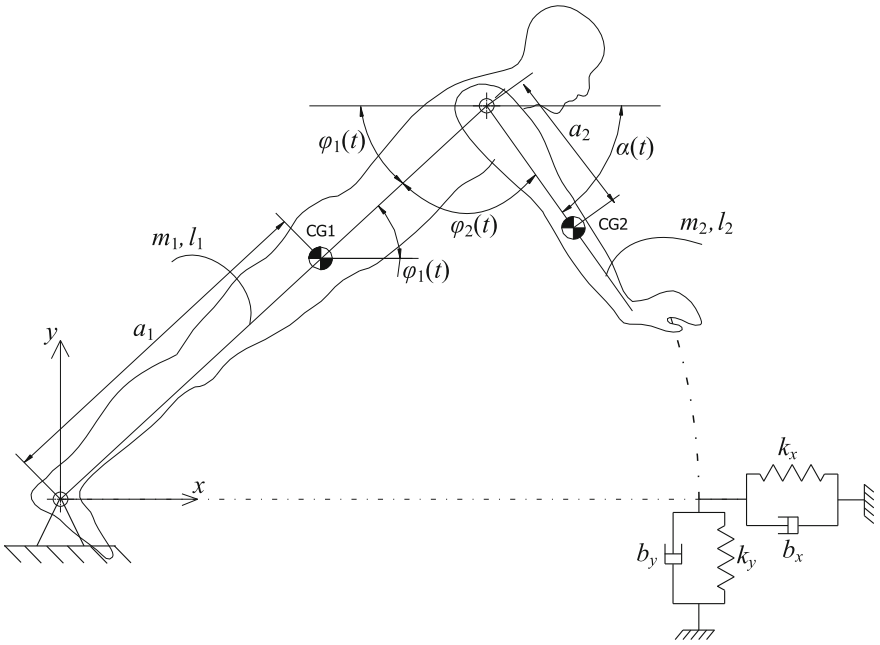

Fig. 1 Model of the investigated biomechanical system

limb. The bodies 1 and 2 have masses m_1, m_2 and moments of inertia about centres of the masses I_1 and I_2, respectively. The appropriate values of the viscous damping coefficients in the joints 1 and 2 equal to c_1 and c_2, respectively, are also included. The equations of motion describing the dynamics of the considered mechanical system have been obtained by the Newton–Euler method. Free Body Diagrams (FBD's) of the considered system are shown in Fig. 2.

In our model, we take the following vectors:

$$\mathbf{r}_{C1}(t) = [x_1(t), y_1(t), 0]^T = [a_1 \cos\varphi_1(t), a_1 \sin\varphi_1(t), 0]^T, \tag{1}$$

$$\mathbf{r}_{C2}(t) = [x_2(t), y_2(t), 0]^T = [l_1 \cos\varphi_1(t) + a_2 \cos\alpha(t), l_1 \sin\varphi_1(t) - a_2 \sin\alpha(t), 0]^T, \tag{2}$$

$$\mathbf{l}_1(t) = [l_1 \cos\varphi_1(t), l_1 \sin\varphi_1(t), 0]^T, \tag{3}$$

$$\mathbf{l}_2(t) = [l_1 \cos\varphi_1(t) + l_2 \cos\alpha(t), l_1 \sin\varphi_1(t) - l_2 \sin\alpha(t), 0]^T, \tag{4}$$

where $\alpha(t) = \pi - \varphi_1(t) - \varphi_2(t)$.

The forces $\mathbf{Q}_1 = [0, -m_1 g, 0]^T$ and $\mathbf{Q}_2 = [0, -m_2 g, 0]^T$ are the gravity forces acting on the centre of gravity of bodies 1 and 2, respectively, where g denotes gravity coefficient ($g = 9.81\ \mathrm{m \cdot s^{-2}}$). The force $\mathbf{R}(t) = [R_x(t), R_y(t), 0]^T$ is the join 1 reaction

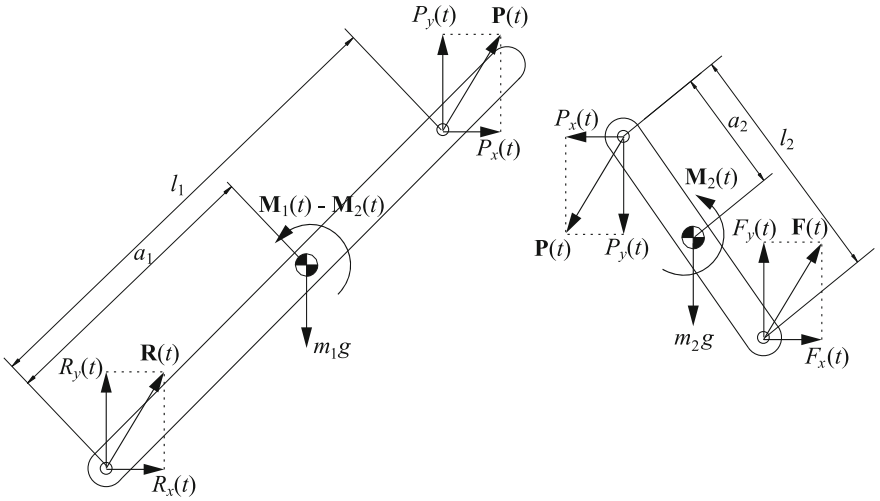

Fig. 2 Free body diagrams of the considered biomechanical system

force. The unknown joint force presented in the free-body diagrams (Fig. 2) is denoted as $\mathbf{P}(t) = [P_x(t), P_y(t), 0]^T$. In turn, the force $\mathbf{F}(t) = [F_x(t), F_y(t), 0]^T$ is the ground reaction force. Next, let $\mathbf{M}_1(t) = [0, 0, 0]^T$ and $\mathbf{M}_2(t) = [0, 0, M_{2z}(t)]^T$ denote the torques generated in joints 1 and 2, respectively. Then, for two considered in Fig. 2 free bodies, we can write down the following equations of motion in vector form.

For body 1, we have

$$m_1 \ddot{\mathbf{r}}_{C1}(t) = \mathbf{R}(t) + \mathbf{Q}_1 + \mathbf{P}(t), \tag{5}$$

$$I_1\ddot{\varphi}_1(t) + c_1\dot{\varphi}_1(t) = \mathbf{M}_1(t) - \mathbf{M}_2(t) + \boldsymbol{\tau}_{\mathbf{R}}(t) + \boldsymbol{\tau}_{\mathbf{P}1}(t), \tag{6}$$

and for body 2 we have

$$m_2 \ddot{\mathbf{r}}_{C2}(t) = -\mathbf{P}(t) + \mathbf{Q}_2 + \mathbf{F}(t), \tag{7}$$

$$I_2\ddot{\varphi}_2(t) + c_2\dot{\varphi}_2(t) = \mathbf{M}_2(t) + \boldsymbol{\tau}_{\mathbf{P}2}(t) + \boldsymbol{\tau}_{\mathbf{F}}(t), \tag{8}$$

where

$$\begin{aligned} \boldsymbol{\tau}_{\mathbf{R}}(t) &= -\mathbf{r}_{C1}(t) \times \mathbf{R}(t) = \\ &= [0, 0, a_1 R_x(t) \sin\varphi_1(t) - a_1 R_y(t) \cos\varphi_1(t)]^T, \end{aligned} \tag{9}$$

$$\begin{aligned} \boldsymbol{\tau}_{\mathbf{P}1}(t) &= [\mathbf{l}_1(t) - \mathbf{r}_{C1}(t)] \times \mathbf{P}(t) = \\ &= [0, 0, (l_1 - a_1) P_y(t) \cos\varphi_1(t) - (l_1 - a_1) P_x(t) \sin\varphi_1(t)]^T, \end{aligned} \tag{10}$$

$$\begin{aligned}\boldsymbol{\tau}_{\mathbf{P}2}(t) &= -[\mathbf{l}_1(t) - \mathbf{r}_{C2}(t)] \times \mathbf{P}(t) = \\ &= [0, 0, a_2 P_y(t)\cos\alpha(t) + a_2 P_x(t)\sin\alpha(t)]^T,\end{aligned} \tag{11}$$

$$\begin{aligned}\boldsymbol{\tau}_{\mathbf{F}}(t) &= [\mathbf{l}_2(t) - \mathbf{r}_{C2}(t)] \times \mathbf{F}(t) = \\ &= [0, 0, (l_2 - a_2)F_y(t)\cos\alpha(t) + (l_2 - a_2)F_x(t)\sin\alpha(t)]^T,\end{aligned} \tag{12}$$

are the moments generated by the forces $\mathbf{R}(t)$, $\mathbf{P}(t)$ and $\mathbf{F}(t)$, respectively. Writing down this vector form equation in the scalar form we obtain the following system of differential equations:

$$\begin{cases} m_1\ddot{x}_1(t) = R_x(t) + P_x(t) \\ m_1\ddot{y}_1(t) = R_y(t) - m_1 g + P_y(t) \\ I_1\ddot{\varphi}_1(t) + c_1\dot{\varphi}_1(t) = -M_{2z}(t) + a_1 R_x(t)\sin\varphi_1(t) - a_1 R_y(t)\cos\varphi_1(t) + \\ \quad + (l_1 - a_1)P_y(t)\cos\varphi_1(t) - (l_1 - a_1)P_x(t)\sin\varphi_1(t) \\ m_2\ddot{x}_2(t) = -P_x(t) + F_x(t) \\ m_2\ddot{y}_2(t) = -P_y(t) - m_2 g + F_y(t) \\ I_2\ddot{\varphi}_2(t) + c_2\dot{\varphi}_2(t) = M_{2z}(t) + a_2 P_y(t)\cos\alpha(t) + a_2 P_x(t)\sin\alpha(t) + \\ \quad + (l_2 - a_2)F_y(t)\cos\alpha(t) + (l_2 - a_2)F_x(t)\sin\alpha(t). \end{cases} \tag{13}$$

Equation (13) can be written in the form

$$\begin{aligned} I_1\ddot{\varphi}_1(t) + c_1\dot{\varphi}_1(t) = &-M_{2z}(t) + a_1 R_x(t)\sin\varphi_1(t) - a_1 R_y(t)\cos\varphi_1(t) + \\ &+ (l_1 - a_1)P_y(t)\cos\varphi_1(t) - (l_1 - a_1)P_x(t)\sin\varphi_1(t), \end{aligned} \tag{14}$$

$$\begin{aligned} I_2\ddot{\varphi}_2(t) + c_2\dot{\varphi}_2(t) = &M_{2z}(t) + a_2 P_y(t)\cos\alpha(t) + a_2 P_x(t)\sin\alpha(t) + \\ &+ (l_2 - a_2)F_y(t)\cos\alpha(t) + (l_2 - a_2)F_x(t)\sin\alpha(t), \end{aligned} \tag{15}$$

where

$$P_x(t) = F_x(t) - m_2\ddot{x}_2(t), \tag{16}$$

$$P_y(t) = F_y(t) - m_2\ddot{y}_2(t) - m_2 g, \tag{17}$$

$$R_x(t) = m_1\ddot{x}_1(t) - P_x(t) = m_1\ddot{x}_1(t) + m_2\ddot{x}_2(t) - F_x(t), \tag{18}$$

$$R_y(t) = m_1\ddot{y}_1(t) + m_1 g - P_y(t) = m_1\ddot{y}_1(t) + m_2\ddot{y}_2(t) + m_1 g + m_2 g - F_y(t). \tag{19}$$

At the time of stumble over an obstacle, human instinctively hold out his hands quickly to the front to fall on them and in this way to absorb the fall. With a rough approximation, it can be assumed that a human hold his hands quickly to such a position φ_0 that at the moment of the fall, they are adjusted approximately perpendicular to the axis of the body ($\varphi_0 \approx 90°$). Due to the hands moment of inertia

the time needed for hold out both hands it is non-zero, so we assumed angle graph $\varphi_2(t)$ as

$$\varphi_2(t) = \varphi_0(1 - e^{-\lambda t}), \tag{20}$$

where φ_0 denotes the angle between torso with legs and hands, while constant parameter λ corresponds to "speed" hold out the hands by human. Knowing the function graph $\varphi_2(t)$ on the basis of Eq. (15) the torque generated by human hands at their extraction in the process of falling can be calculated as follows:

$$\begin{aligned} M_{2z}(t) &= I_2\ddot{\varphi}_2(t) + c_2\dot{\varphi}_2(t) - a_2P_y(t)\cos\alpha(t) + \\ &- a_2P_x(t)\sin\alpha(t) - (l_2 - a_2)F_y(t)\cos\alpha(t) - (l_2 - a_2)F_x(t)\sin\alpha(t). \end{aligned} \tag{21}$$

Finally, substituting Eqs. (21) to (14) gives one differential equation for the rotation of the body 1, whose the solution is function $\varphi_1(t)$.

Ground reaction forces modelling

At the end of the second body the force $\mathbf{F}(t)$ is applied, which corresponds to the force resulting from impact. This force occurs only in the contact point of the ground (with no contact this force is zero). The force $\mathbf{F}(t)$ is applied at the tip of body 2 meaning the end of the second link (point hand contact with the ground). In a real system the connection between the parts of the human body are stiffness and damped. Damping forces in assumed model are not included, but this behaviour of real joints is modelled as ground stiffness and damping, which followed the fall of the human body. The stiffness and damping parameters of the ground are chosen such that the obtained numerical results coincide with the experimental results presented in the literature.

The impact force, including stiffness and damping of the ground, is taken into account in the following form

$$F_x(t) = -[k_x(x(t) - x_0) + b_x\dot{x}(t)] \cdot \mathbf{1}(-y(t)), \tag{22}$$

$$F_y(t) = -[k_y y(t) + b_y\dot{y}(t)] \cdot \mathbf{1}(-y(t)), \tag{23}$$

where k_x, k_y are ground stiffness coefficients, b_x, b_y are ground viscous damping coefficients, $x_0 = \sqrt{l_1^2 + l_2^2 - 2l_1l_2\cos\varphi_0}$, $x(t) = l_1\cos\varphi_1(t) + l_2\cos\alpha(t)$, $y(t) = l_1\sin\varphi_1(t) - l_2\sin\alpha(t)$, and the function $\mathbf{1}(-y(t))$ is the step function defined as follows:

$$\mathbf{1}(-y(t)) = \begin{cases} 1 & \text{if} \quad y(t) < 0, \\ 0 & \text{if} \quad y(t) \geq 0. \end{cases} \tag{24}$$

The initial conditions

To carry out numerical simulation of the proposed mathematical model initial conditions $\varphi_1(0)$ and $\dot{\varphi}_1(0)$ are required. Assuming that before stumbling human

has hands stacked along the torso, we take $\varphi_1(0) = \pi/2$ (see Fig. 1). In turn, the initial velocity $\dot{\varphi}_1(0)$ is estimated based on the linear velocity v_0 of human motion at the moment of stumbling, and assuming that the rotation of his body takes about a fulcrum feet (see Fig. 1). The principle of conservation of momentum yields

$$(m_1 + m_2)(0 - v_0) = F\Delta t, \tag{25}$$

where $F\Delta t$ is an impulse force that causes rotation of the human at the moment of stumbling an obstacle. In turn, rotational motion of a human body around the axis of rotation (around the legs) is governed by the equation

$$I\frac{\Delta\varphi_1(t)}{\Delta t} = rF \Rightarrow \Delta\varphi_1(t) = -\frac{(m_1 + m_2)v_0 r}{I} = \dot{\varphi}_1(0), \tag{26}$$

where I is the moment of inertia of the human around the legs axis with his hands adjusted along the body, and r is the distance of the centre of human gravity in a standing position with hands adjusted along the body from the ground.

3 Simulation Results

The results of numerical simulations were obtained using Mathematica 10 software. In order to determine the centre of gravity of a component of the human parts and the moments of inertia, one can employ the proper command of the programs AutoDesk Inventor. The full 3D scanned human body model is presented in Fig. 3 due to courtesy of Rory Craig (GrabCAD) [12]. Even though human body does not consist of a homogenous structure, the value of the mass is calculated assuming the average density $\rho = 1050\ \mathrm{kg \cdot m^{-3}}$. Parameters used in numerical simulations are presented in Table 1. The simulations presented in Figs. 4, 5, 6, 7 and 8 are carried out for the fixed ground parameters: $k_x = k_y = k = 16\ 000\ \mathrm{N \cdot m^{-1}}$ and $b_x = b_y = b = 1\ 000\ \mathrm{N \cdot s \cdot m^{-1}}$.

Figure 4 shows a times histories of force $F_y(t)$ acting on the single hand for $v_0 = 0$, $\lambda = 4\ \mathrm{s^{-1}}$ and for the different angle ϕ_{Arm} between the arm and normal axis of the ground. In the case of free fall of the human body the influence of the angle ϕ_{Arm} at the moment of the fall on the $F_{y\max}$ can be neglected. Small differences in larger values of force $F_{y\max}$ and shorter time falling are caused by the higher amount of torque generated by human hands $M_{2z}(t)$, which is transformed to the human body and causes its rotation about a support point.

The results presented in Figs. 5 and 6 show the influence of different values of the velocity v_0 and parameter λ on time histories of force $F_y(t)$.

Figure 5 shows that for larger values the parameter λ, the time of falling process on the ground is lower, but this has no significant impact on the force $F_{y\max}$.

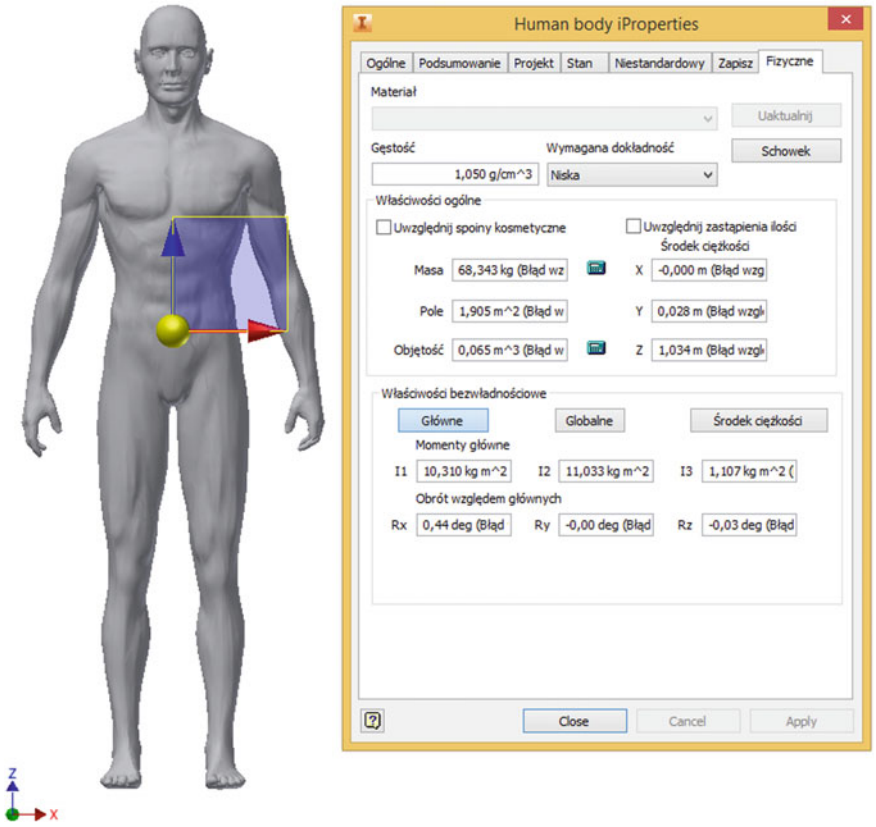

Fig. 3 Calculation of parameters for the human body [12]

Table 1 Body segment lengths, masses, moments of inertia and damping coefficients

		Value	Unit
Parameters	a_1; a_2	1.01; 0.22	m
	l_1; l_2; r	1.4; 0.53; 1.03	m
	m_1; m_2	61.0; 7.4	kg
	I_1; I_2; I	9.9; 0.232; 10.3	kg · m^2
	c_1; c_2	0.1; 0.1	N · m · s

Figure 6 shows that the initial value of the speed of the falling of human is much higher. Furthermore, in this case, ($v_0 = 2\ \mathrm{m \cdot s^{-1}}$) the influence of the parameter λ is higher than for the case of velocity $v_0 = 0$.

Figures 7 and 8 show the influence of parameters v_0 and λ on times histories of force for different angle values ϕ_{Arm} angles with a simultaneous increase of the velocity v_0 and λ (at higher initial velocity value of human hold out hands). As might be expected, higher initial velocities v_0 imply a rapid human fall on the

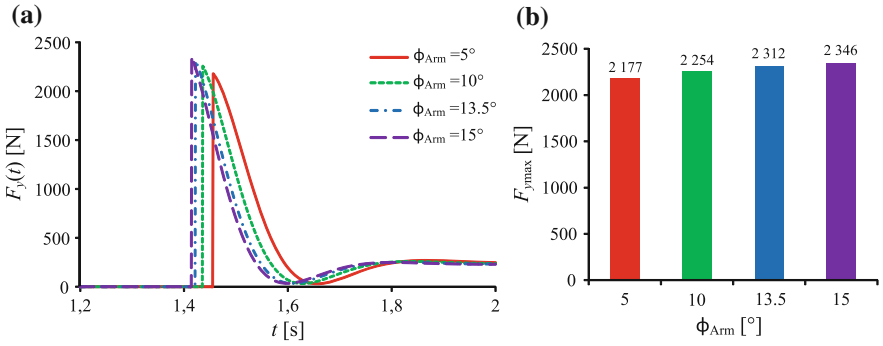

Fig. 4 Time histories of contact force $F_y(t)$ **a** and its maximum values F_{ymax} **b** for different angle ϕ_{Arm} ($v_0 = 0$, $\lambda = 4\ s^{-1}$)

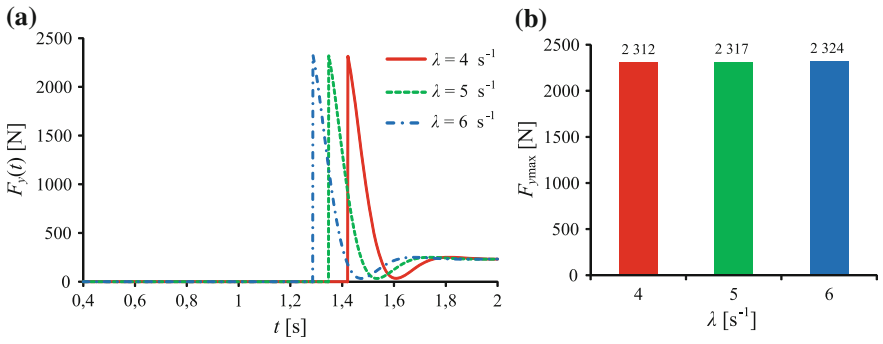

Fig. 5 Time histories of contact force $F_y(t)$ **a** and its maximum values F_{ymax} **b** for different parameters λ ($\phi_{Arm} = 13.5°$, $v_0 = 0$)

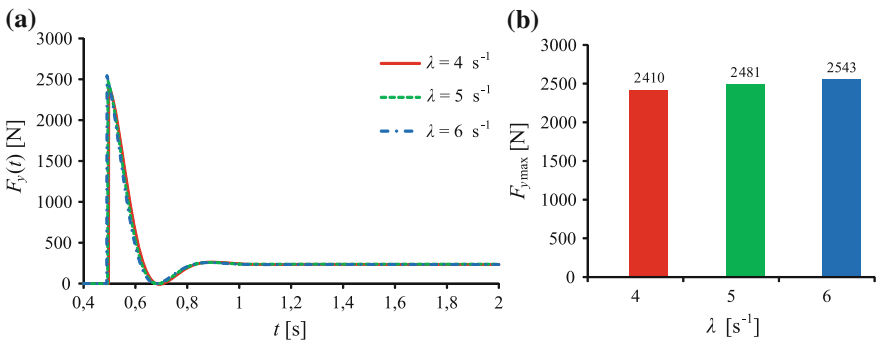

Fig. 6 Time histories of contact force $F_y(t)$ **a** and its maximum values F_{ymax} **b** for different parameters λ ($\phi_{Arm} = 13.5°$, $v_0 = 0$)

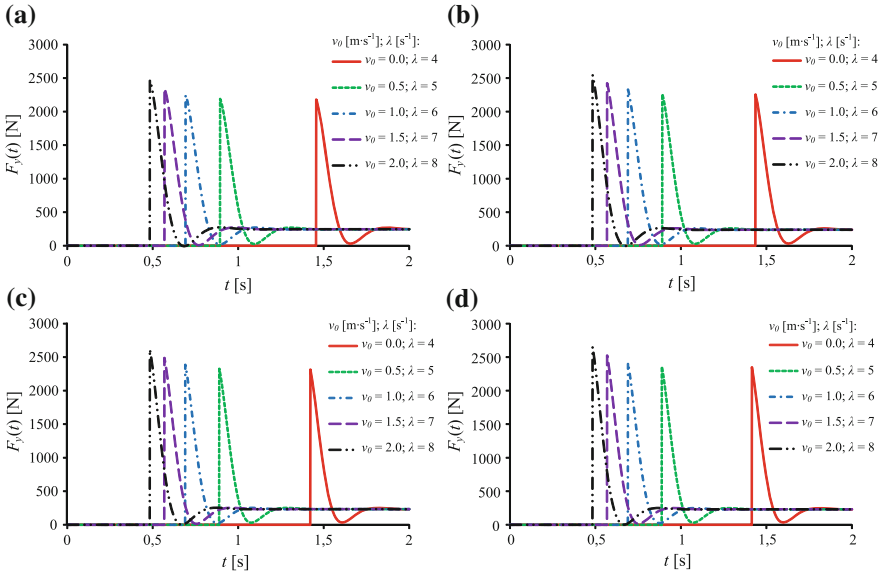

Fig. 7 Time histories of contact force $F_y(t)$ for different values of parameters v_0 and λ. **a** $\phi_{\text{Arm}} = 5°$, **b** $\phi_{\text{Arm}} = 10°$, **c** $\phi_{\text{Arm}} = 13.5°$, **d** $\phi_{\text{Arm}} = 15°$

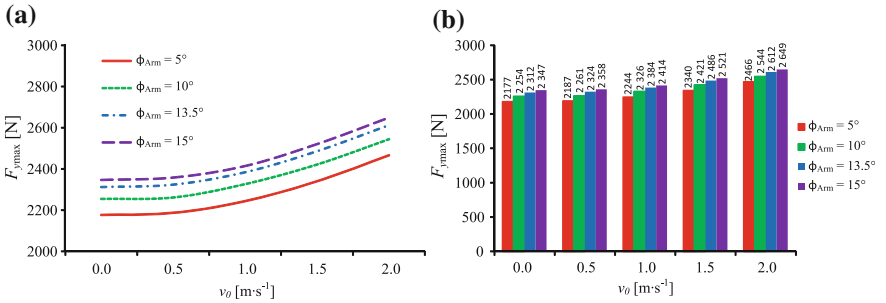

Fig. 8 Maximum values $F_{y\max}$ of contact force as a function of velocity v_0 for different angles ϕ_{Arm}

ground and influence of the angle ϕ_{Arm} has also an impact on the force $F_{y\max}$ (Fig. 9).

In what fallows we study the impact of ground parameters (stiffness and damping) on the obtained results. The following parameters are fixed: $\phi_{\text{Arm}} = 13.5°$, $v_0 = 2\ \text{m} \cdot \text{s}^{-1}$ and $\lambda = 8\ \text{s}^{-1}$. As can be seen, the highest effect on the maximum force value $F_y(t)$ has damping of the ground. It follows from the fact that when human hand is in a contact with the ground, the force of the damping is activated by the ground, which is proportional to the impact velocity with the coefficient of proportionality b. Component of the force $F_y(t)$ associated with the ground stiffness

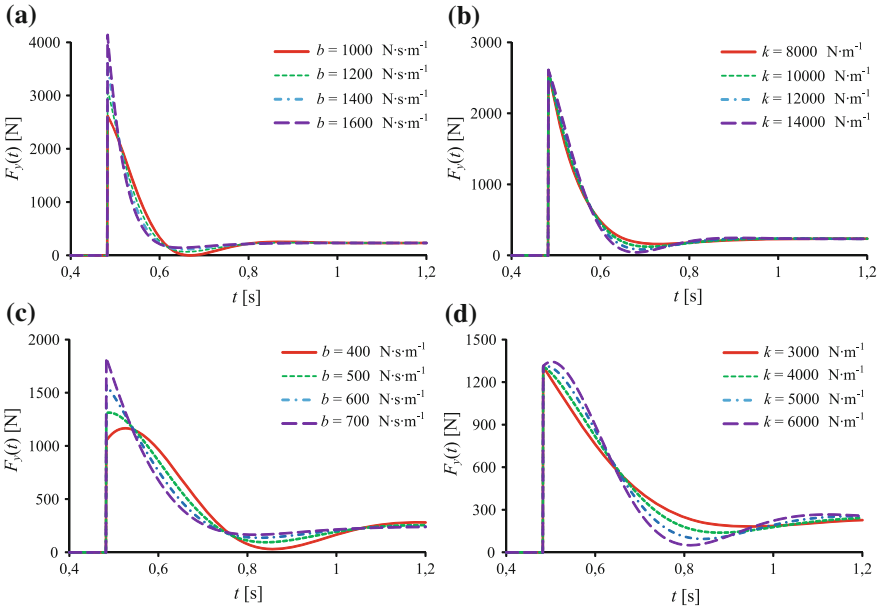

Fig. 9 Time histories of contact force $F_y(t)$ for different values of parameters b and k ($\phi_{\text{Arm}} = 13.5°$, $v_0 = 2\ \text{m} \cdot \text{s}^{-1}$, $\lambda = 4\ \text{s}^{-1}$). **a** $k = 16000\ \text{N} \cdot \text{m}^{-1}$. **b** $b = 1000\ \text{N} \cdot \text{s} \cdot \text{m}^{-1}$. **c** $k = 5000\ \text{N} \cdot \text{m}^{-1}$. **d** $b = 500\ \text{N} \cdot \text{s} \cdot \text{m}^{-1}$

k does not essentially affect the value of the maximum $F_{y\max}$ (it increases from zero at the time of hand contact with the ground, proportionally to the penetration depth into the ground.

4 Conclusions

This paper presents a relatively simple mechanical model governing the forward fall on outstretched hands. The considered model is constructed based on a mechanical system with two degrees of freedom and classical impact notion. Numerical simulations are performed for the parameters obtained based on the scanning computer model of the human body. In turn, biochemical properties of the human cartilage joint are modelled by the properties of the ground stiffness and damping. As it is shown, the obtained results fit well with experimental results presented in the literature, both from a qualitative and quantitative point of view. In particular, the model allows to estimate magnitude of contact force in various scenarios of falling process. The numerical simulations show that the essential influences on the obtained results have not only parameters describing the human body, but also the parameters modelling the ground. Although the proposed model is relatively simple, it has been validated by numerical computations. Further modifications and

improvements of the proposed model relies on taking into account the stiffness and damping in each of the joints as well as through increase of the number of degrees of freedom of the human body. These issues will be the subject of our further investigations related to the problem of the forward fall on the outstretched hands.

Acknowledgments The work has been supported by the National Science Centre of Poland under the grant OPUS 9 no. 2015/17/B/ST8/01700 for years 2016–2018.

References

1. Nevitt, M.C., Cummings, S.R.: Type of fall and risk of hip and wrist fractures: the study of osteoporotic fractures. J. Am. Geriatr. Soc. **41**, 1226–1234 (1993)
2. Chiu, J., Robinovitch, S.N.: Prediction of upper extremity impact forces during fall on the outstretched hand. J. Biomech. **31**, 1169–1176 (1998)
3. DeGoede, K.M., Ashton-Miller, J.: Biomechanical simulations of forward fall arrest: effects of upper extremity arrest strategy, gender and aging-related declines in muscle strength. J. Biomech. **36**, 413–420 (2003)
4. Kim, K.J., Ashton-Miller, J.: Segmental dynamics of forward fall arrest: a system identification approach. Clin. Biomech. **24**, 348–354 (2009)
5. Lehner, S., Geyer, T., Michel, F.I., Schmitt, K.U., Senner, V.: Wrist injuries in snowboarding—simulations of a worst case scenario of snowboard falls. Procedia Engineering **72**, 255–260 (2014)
6. Biesiacki, P., Awrejcewicz, J., Mrozowski, J., Woźniak, K.: Nonlinear biomechanical analysis of the human upper limb in a outstretched forward fall. In: Awrejcewicz, J., Kaźmierczak, M., Olejnik, P., Mrozowski, J. (eds.) Dynamical Systems–Applications. Publishing House of Lodz University of Technology, pp. 229–240 (2013)
7. Biesiacki, P., Mrozowski, J., Awrejcewicz, J.: Study of dynamic forces in human upper limb in forward fall. In: Awrejcewicz, J., Kaźmierczak, M., Mrozowski, J., Olejnik, P. (eds.) Dynamical Systems—Applications. Publishing House of Lodz University of Technology, pp. 65–76 (2015)
8. Silva, M., Barbosa, R., Castro, T.: Multi-legged walking robot modelling in MATLAB/Simmechanics™ and its simulation. In: Proceedings of the 2013 8th EUROSIM Congress on Modelling and Simulation, EUROSIM, Cardiff, Wales, pp. 226–231, 10–13 Sept 2013
9. Yamaguchi, G.T.: Dynamic Modelling of Musculoskeletal Motion: Springer-Science + Business Media, B.V. (2001)
10. Anderson, F.C., Pandy, M.G.: Dynamic optimization of human walking. J. Biomech. Eng. **123**, 381–390 (2001)
11. Neptune, R.R., Wright, I.C., van den Bogert, A.J.: A method for numerical simulation of single limb ground contact events: application to heel–toe running. Comput. Methods Biomech. Biomed. Eng. **3**, 321–334 (2000)
12. GrabCAD: Open CAD library (2016). https://grabcad.com/library